Journal of Wind Engineering and Industrial Aerodynamics, 46 & 47 (1993) 213–218
Elsevier

Large-eddy-simulation of the flow around building models

W. FRANK+
Institut fuer Stroemungslehre und Stroemungsmaschinen, Universitaet Karlsruhe, Kaiserstrasse 12, D-W-7500 Karlsruhe-1, Germany
H. MAUCH
ABB-Turbo Systems ZTL 21, CH-5401 Baden, Switzerland

Abstract

In the paper a numerical program package is described to calculate incompressible, unsteady, three-dimensional, viscous and turbulent flow fields around sharp edged obstacles. By this the velocity and pressure distributions in the flow field and on the surfaces of square-formed bodies in a plane channel can be determined, as well as the frequencies of periodic vortex separations.

The channel consists of two plates extended to infinity. On the lower plate the square-formed body, which is identical with the building model, is placed. The flow is maintained by a pressure gradient in x_1-direction. Therefore the main flow direction is identical with the x_1-direction, see figure 1.

The purpose of our work is to apply the concept of large-eddy-simulation (LES) to practical problems in building aerodynamics. By the aid of numerical calculations some special situations for the experimental investigation of the flow around building models in a wind tunnel are demonstrated. The numerical results are compared with different experiments.

1. BASIC EQUATIONS AND DISCRETISATION

In order to calculate turbulent flow fields at high Reynolds numbers, which usually occur in practical problems in building aerodynamics, a turbulence model is necessary. We use the large-eddy-simulation (LES). In this case the basic equations are changed due to smoothing operations. In the large-eddy-simulation the large scales, depending on the type of the flow, are simulated directly. The information on the small, not resolved scales, are given by the model assumptions for the subgrid scale turbulence. The separation of the large scales from the subgrid scale effects are made by the integration of the basic equations over small volume elements. The size of these elements are given by the mesh grid. Hereby we get the following normalized basic equations in difference form:

$$\delta_i \, {}^{i}\overline{v_i} = 0$$

$$\overset{v}{\left(\frac{\partial \overline{v_i}}{\partial t} \right)} = -\delta_j \left({}^{j}\overline{v_i} \, {}^{i}\overline{v_j} \right) - \delta_i \, {}^{i}\overline{p} + \delta_j \overset{j}{\left(\overline{\nu \left(\frac{\partial v_i}{\partial x_j} + \frac{\partial v_j}{\partial x_i} \right)} - {}^{\prime}\overline{v_i' \, v_j'} \right)} + \delta_{1i} \, P_x$$

+ to whom correspondence should be sent

These equations are solved numerically on a staggered grid. For the spatial discretisation central finite differences are used.

2. TIME INTEGRATION AND SUBGRID SCALE MODELLING

For the time integration an explicit Euler-leap-frog scheme is applied. Due to the difficulties in calculating the pressure term in the above-mentioned system of differential equations (the operation divergence applied to the momentum equation results in an elliptic differential equation with inhomogeneous Neumann-type boundary conditions) the solution procedure follows the scheme of Corin /3/. By this in a first step an approximated velocity field is calculated without taking in consideration the turbulent pressure term. In the next step we have to solve a Poisson-equation for the pressure term in order to determine finally the exact velocity field. The described set of equations has to be solved at every time step. This demonstrates that the solution of the discrete Poisson-equation is an essential part of the numerical calculation. Therefore we have to introduce fast Poisson solvers and to use the capacitance matrix technique (CMT) (see e.g. Buzbee et al. /1/, Schumann /8/, Schmitt /6/) to minimize the CPU-time.

In large-eddy-simulations the subgrid scale stresses are to simulate. For this purpose the unknown subgrid scale stresses can be devided into an unsteady, local-isotropic part and into a steady inhomogeneous part, as proposed by Grötzbach /5/ and Schumann /7/. For both parts the Boussinesq-approximation is carried out. The simulation of the isotropic eddy viscosity is done by the energy model of Prandtl. For the inhomogeneous term of the eddy viscosity the simpler Prandtl mixing-length-model is applied.

Since the basic equations are of the elliptic type on all boundaries of the calculation region, boundary conditions have to be defined. We use in x_1- and x_2-direction periodic boundary conditions. On the channel walls and on the surfaces of the building model no-slip conditions are assumed. The size of the calculation domain is 128x64x64 grid points (x_1-, x_2-, x_3-direction).

3. RESULTS

Figure 2 shows a comparison of the calculated velocity profiles with experiments for a turbulent flow. In both pictures the time-averaged velocity components in x_1-direction are plotted: in the upper half as sideview and in the lower half as topview. The numerical results are compared with experiments (marked with + in the plots) carried out by Castro and Robins /2/. On the top of the building model as well as in the leeward region behind the model a good agreement between the numerical results and the experimental data can be seen.

Also the high location of the vortex center, which is observed in the experiments, is well predicted by the numerical calculation (see figure 3). In this figure the calculated velocity distribution around the building model are plotted; in the upper half the v_1-, v_3-components of the velocity vectors and in the lower half the v_1-profiles.

Figure 4 shows the comparison of the experimentally determined streaklines (above) on the ground plate of the wind tunnel with the numerical results (below). From

the comparison can be seen that the large-eddy-simulation describes very well details of the turbulent flow field: the horse-shoe vortex around the building model, the flow separation at the side walls of the model and the details in the wake of the body.

For the flow around slender bodies often appear periodic load fluctuations due to unsteady vortex separation. These instabilities can lead on the surfaces of a building to a material damage. Therefore the frequencies of such a vortex separation is of great interest for practical problems in building aerodynamics. In figures 5 and 6 the flow around a sharp-edged rectangular cylinder at six different time steps for one period are shown. In figure 5 we see the velocity distributions and in figure 6 the momentaneous streamlines are plotted. The vortex separation is alternating, that means it is displaced at about half a period.

In figure 7 the calculated Strouhal numbers for different Reynolds numbers are compared with other numerical and experimental results.

An important help for the evaluation of the three-dimensional numerical results are the representation of the streamlines. In figure 8 the three-dimensional streamlines for the flow around a rectangular cylinder in a channel are drawn in the so-called "Kavalier"-perspective (above), in the sideview (center) and in the view from above (below). On this figure the additional influence of the top wall and the ground plate of the wind tunnel to the flow phenomena is shown. In the immediate neighbourhood of the walls the fluctuations in the flow are strongly influenced; there is no periodic unsteady flow in this region. The unsteady flow phenomena appear only in some distance from the tunnel walls. For the interpretation of such pictures the top- and sideviews together with the 3-D representation must be taken into account to be sure that no misinterpretation is made.

4. REFERENCES

1. Buzbee, B.L.; Dorr, F.W.; George, J.A. and G.H Golub, The direct solution of the discrete Poisson equation on irregular regions, SIAM J. on numerical analysis 8 (1971), pp. 722-736.
2. Castro, I.P. and A.G. Robins, The flow around a surface-mounted cube in uniform and turbulent streams, J. Fluid Mech. 79 (1977), pp. 307 - 335.
3. Chorin, A.J., Numerical solution of the Navier-Stokes equations, Math.Comp. 22 (1968), pp. 745 - 762.
4. Franke, R. and B. Schönung, Numerische Simulation der laminaren Wirbelablösung an Zylindern mit quadratischen oder kreisförmigen Querschnitten, SFB-210/T/39-Report, University of Karlsruhe (1988).
5. Grötzbach, G., Direkte numerische Simulation turbulenter Geschwindigkeits-, Druck- und Temperaturfelder bei Kanalströmungen, Ph.D. Thesis, University of Karlsruhe (1977).
6. Schmitt, L., Grobstruktursimulation turbulenter Grenzschicht-, Kanal- und Stufenströmungen, Ph.D. Thesis, Techn. University of Munich (1988).
7. Schumann, U., Ein Verfahren zur direkten Simulation turbulenter Strömungen in Platten- und Ringspaltkanälen und über seine Anwendung zur Untersuchung von Turbulenzmodellen, Ph.D. Thesis, University of Karlsruhe (1973).
8. Schumann, U., Fast elliptic solvers and their application in fluid dynamics, in: Comp. Fluid Dyn., ed. W. Kollmann, Hemisphere Publ. Corp. (1971), pp. 401-430.

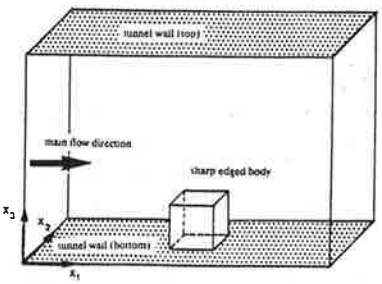

Fig.1 Sketch of the tunnel geometry and the building model

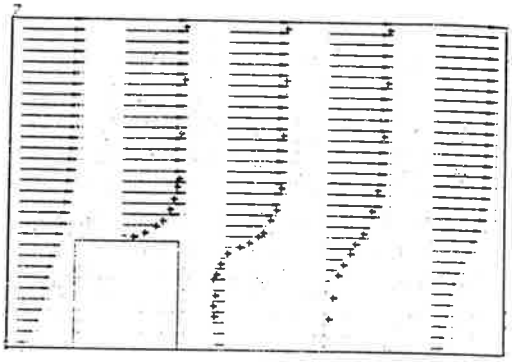

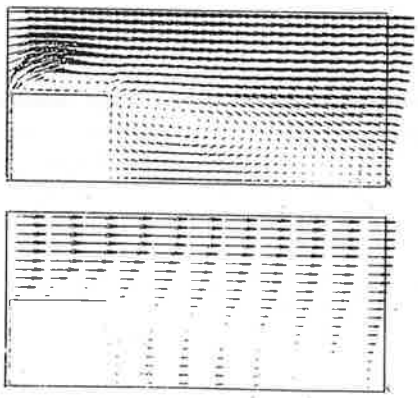

Fig.3

Calculated turbulent velocity

top: v_1-, v_3-components,
bottom: v_1-profiles

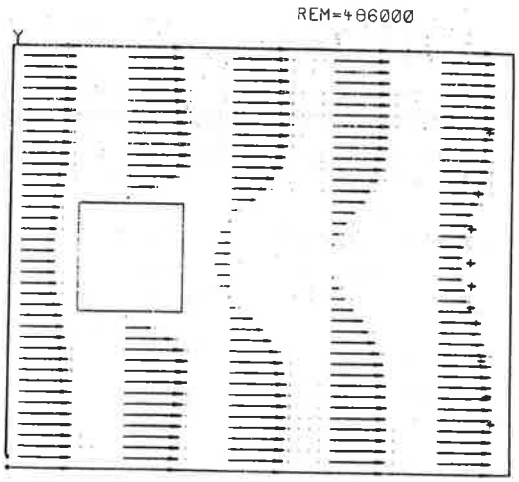

Fig.2 Comparison of the calculated time-avaraged velocity profiles with experimental data. (+ = experiment)

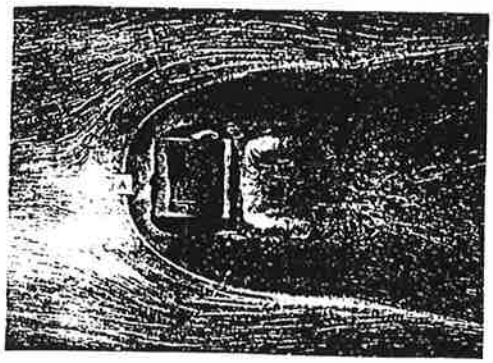

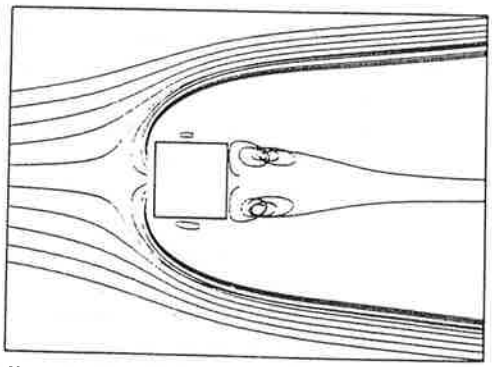

Fig.4 Comparison of the visualized streaklines in the wind tunnel with calculated streamlines in the plane k=1.

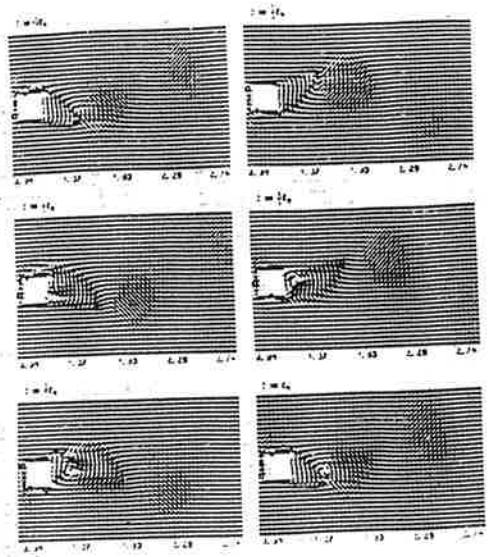

Fig.5 Periodic flow separation behind a square cylinder at Re = 40.000. Calculated velocity vectors (topview).

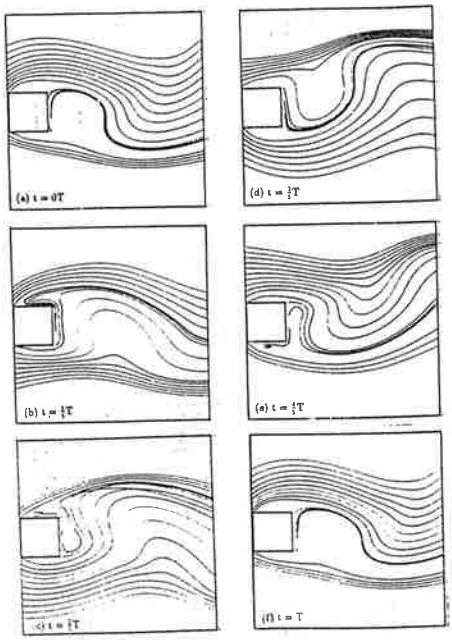

Fig.6 Periodic flow separation behind a square cylinder at Re = 40.000. Calculated momentaneous streamlines (topview).

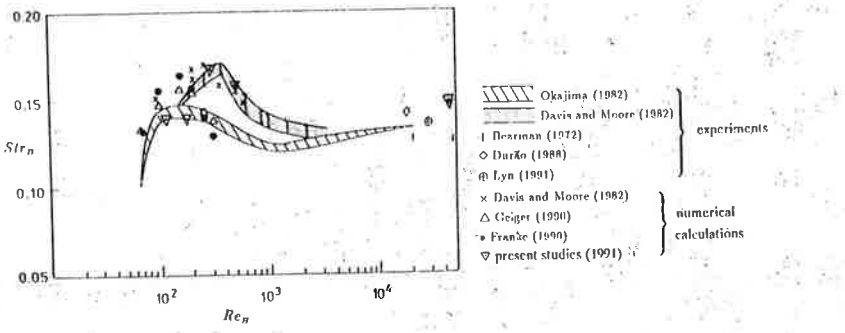

Fig.7 Strouhal-number versus Reynolds-number for the flow around square cylinders from /4/.

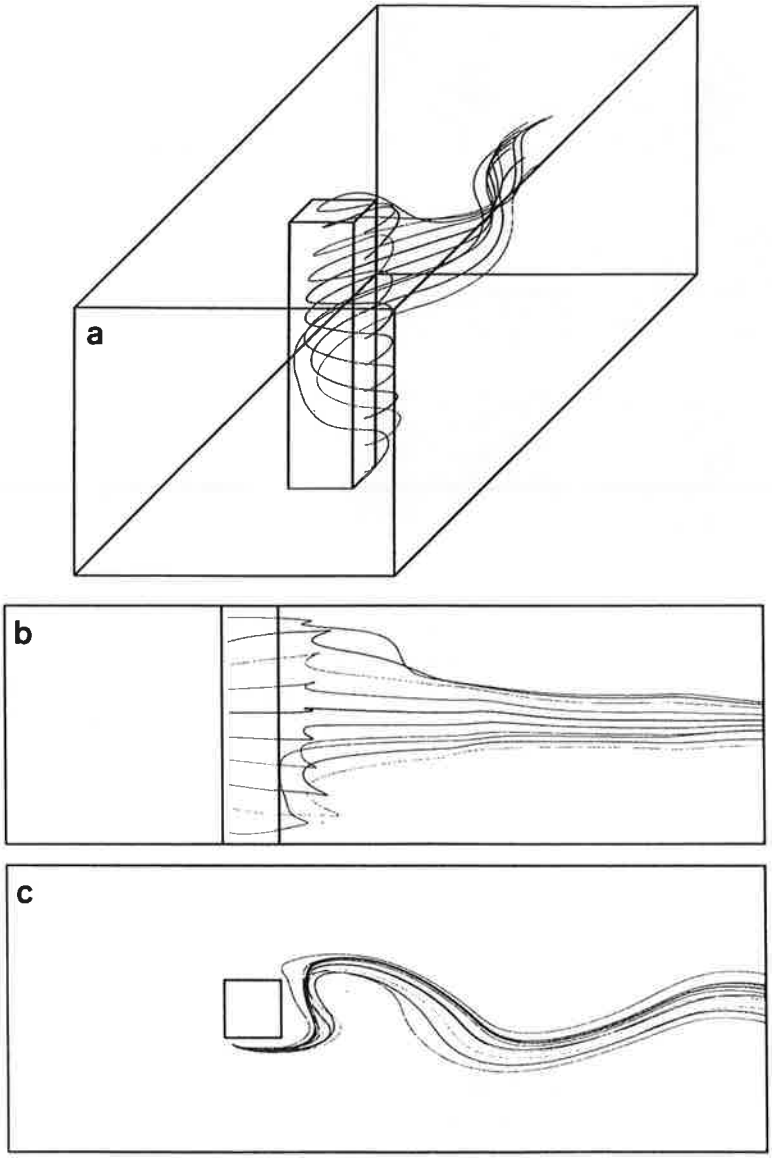

Fig.8 Particle pathes calculated from the momentaneous velocity field for a square cylinder (Re = 139).
a) perspective drawing b) sideview c) topview